Precipitation trends in version 2 of the Canadian Homogenized Monthly Precipitation Dataset

Xiaolan L. Wang, Yang Feng, Francis W. Zwiers & Vincent Y. S. Cheng

2026

Pacific Climate Impacts Consortium (PCIC)

PCIC Publications

Original citation:

Wang, X. L., Feng, Y., Zwiers, F. W., & Cheng, V. Y. S. (2026). Precipitation trends in version 2 of the Canadian Homogenized Monthly Precipitation Dataset. *Atmosphere-Ocean*, 1–16. https://doi.org/10.1080/07055900.2026.2617861

Precipitation Trends in Version 2 of the Canadian Homogenized Monthly Precipitation Dataset

Xiaolan L. Wang [1,*], Yang Feng[1], Francis W. Zwiers[2], and Vincent Y. S. Cheng [1]

[1]*Climate Research Division, Environment and Climate Change Canada, Victoria, Canada*
[2]*Pacific Climate Impacts Consortium, University of Victoria, Victoria, Canada*

[Original manuscript received 11 July 2025; accepted 6 January 2026]

ABSTRACT *This paper describes the development of two improved Canadian homogenized monthly precipitation datasets, the CanHomP mlyV2 station dataset, which includes the entire data record of 425 long-term stations across Canada (since 1840 or later), and its gridded version CanGridP mlyV2, which covers the entire Canadian land mass for the 1949–2023 period and southern Canada for 1916–2023. The latter is subsequently used to provide updated estimates of Canada's historical precipitation trends with an assessment of trend representativeness. The V2 datasets benefit from the use of improved station data and metadata and an improved data homogenization procedure, which together result in better spatial consistency of trends than seen in unhomogenized data. Estimates of precipitation trends based on CanGridP mlyV2 also exhibit temperature scaling rates that are more in line with physical expectations than the previous versions of gridded precipitation datasets, which exhibited unphysically high temperature scaling rates. Precipitation is estimated to have increased in most areas from southern Nunavut to the Arctic Archipelago and from Labrador to northeastern Quebec in all seasons. It has also increased in a zonal band around 62°N in summer, and in most areas in British Columbia and along the St. Lawrence River in spring and autumn. The most outstanding variation of trends in seasonal precipitation is seen in a broad band across southern Canada, where winter precipitation has decreased significantly without extensively significant changes in the other seasons. The best estimate of increase in the period 1949–2023 is 9.7% for Canada as a whole, 18.9% for Canada's North, and 7.5% for Canada's South. The estimated rate of change in Canada's annual precipitation expressed as a function of surface air temperature change is 4.9% per 1˚C of warming for the period 1949–2023. Over the century-long period 1916–2023, annual precipitation in Canada's South is estimated to have increased 10.7%.*

RÉSUMÉ *[Traduit par la rédaction] Cet article décrit l'élaboration de deux ensembles de données homogénéisées sur les précipitations mensuelles au Canada, l'ensemble de données de la station CanHomP mlyV2, qui englobe l'ensemble des données enregistrées par 425 stations à long terme à travers le Canada (depuis 1840 ou plus tard), ainsi que sa version maillée CanGridP mlyV2, qui couvre l'ensemble du territoire canadien pour la période 1949-2023 et le sud du Canada pour la période 1916–2023. Cette dernière est ensuite utilisée pour fournir des estimations actualisées des tendances historiques des précipitations au Canada, accompagnées d'une évaluation de la représentativité des tendances. Les ensembles de données V2 bénéficient de l'utilisation de données et métadonnées améliorées provenant des stations et d'une procédure d'homogénéisation des données améliorée, qui, ensemble, permettent d'obtenir une meilleure cohérence spatiale des tendances que celle observée dans les données non homogénéisées. Les estimations des tendances des précipitations basées sur CanGridP mlyV2 présentent également des taux d'échelle de température plus conformes aux attentes physiques que les versions précédentes des ensembles de données maillées sur les précipitations, qui présentaient des taux d'échelle de température anormalement élevés. On estime que les précipitations ont augmenté dans la plupart des régions, du sud du Nunavut à l'archipel arctique et du Labrador au nord-est du Québec, et ce, pendant toutes les saisons. Elles ont également augmenté dans une bande zonale autour de 62° N en été, ainsi que dans la plupart des régions de la Colombie-Britannique et le long du fleuve Saint-Laurent au printemps et à l'automne. La variation la plus marquée des tendances en matière de précipitations saisonnières s'observe dans une large bande traversant le sud du Canada, où les précipitations hivernales ont considérablement diminué sans que les autres saisons ne connaissent de changements importants. La meilleure estimation de l'augmentation pour la période 1949-2023 est de 9,7 % pour l'ensemble du Canada, de 18,9 % pour le nord du Canada et de 7,5 % pour le sud du Canada. Le taux de variation estimé des précipitations annuelles au Canada, exprimé*

*Corresponding author's email: xiaolan.wang@ec.gc.ca

en fonction de la variation de la température de l'air à la surface, est de 4,9 % par 1 °C de réchauffement pour la période 1949-2023. Au cours de la période centenaire allant de 1916 à 2023, les précipitations annuelles dans le sud du Canada auraient augmenté de 10,7 %.

KEYWORDS precipitation; trend analysis; reanalysis data; climate change; quality control; homogeneity tests; data homogenization

1 Introduction

Precipitation is an essential climate variable (https://gcos.wmo.int/site/global-climate-observing-system-gcos/essential-climate-variables) that has high impact potential on society and the environment. It is non-continuous and highly variable from location to location and from one time point to another, and it can occur in both liquid and frozen forms including rain, snow, hail, freezing rain, etc. Thus, it requires an observing network of higher station density and is much more challenging to measure in comparison with air temperature, especially for northern countries such as Canada where precipitation is often frozen. Precipitation data, which have a non-normal distribution (e.g. Martinez-Villalobos & Neelin, 2019), are more prone to measurement errors than temperature that are also challenging to detect and correct. For example, different quality control procedures are required to identify small-value (0 or near-zero monthly amount) and large-value errors (Cheng et al., 2024).

Environment and Climate Change Canada (ECCC) has devoted much effort to quality control and improve data quality, accuracy and consistency (homogeneity) to make the data suitable for characterizing Canada's precipitation climate and how it has changed over time. Particularly, Wang et al. (2023) developed version 1 of the Canadian Homogenized Monthly Precipitation dataset, CanHoPmlyV1 (available at https://open.canada.ca/data/en/dataset/1dd0c28e-2266-42e2-8985-2f47659e9d02), which consists of 425 long-term monthly precipitation data series that were formed by joining data records from neighbouring stations and homogenizing the joined records. Prior to homogenization, most missing values in the period since 1948 in the 425 data series were infilled with values estimated by advanced interpolation of all available observations at other stations in the region for the month in question.

The objective of this study was to produce version 2 of the Canadian Homogenized Monthly Precipitation dataset, CanHomP mlyV2, with improved source data and improved quality-control and data homogenization methods. The 425 homogenized data series are also extended to the end of 2023. The 425 stations are referred to as CanHomP stations hereafter.

The remainder of this article is arranged as follows. Section 2 describes the improved source datasets used, and Section 3, the improvements in quality control and homogenization methods. Section 4 presents the characteristics and effects of data inhomogeneity, and Section 5 presents precipitation trends estimated from the new monthly precipitation dataset and its gridded version, CanGridP mlyV2. We complete this article with a summary and some discussion in Section 6.

2 Improved source data

a *Station precipitation data*

As indicated in Section 1, this study continues to focus on the 425 stations considered by Wang et al. (2023). They chose these stations for their long-term records of good quality and/or critical locations in data-sparse or complex terrain areas, with consideration of the likelihood that these stations will continue "to be operated and well maintained into the distant future, producing complete data (with few missing values) of good quality for decades to come". At the time of selection a few years ago, all 425 locations had an active automated station, including designated Reference Climate Stations that are specifically designed for climate purposes and are expected to continue operating indefinitely. These criteria were used to ensure longevity and temporal consistency of observations. These 425 long-term daily data series were formed by joining daily precipitation data records from collocated or nearby stations that were extracted mainly from the 2020 version of the Adjusted Daily Rainfall and Snowfall (AdjDlyRS) manual gauge dataset, although adjusted daily precipitation data from a small number of Belfort or Fisher-Porter automated gauges were also used (Wang et al., 2023). As detailed in Wang et al. (2023), criteria for choosing the best nearby stations to join to form a long-term data series include the similarity between the stations (correlation between the first-order difference series), as well as the length and completeness and quality of data record. Although the search radius was 300 km, 94.6% and 99.6% of the joined stations are within 100 and 200 km radius, respectively (Wang et al., 2023). We update the joined data series to the end of 2023, including updates to the station joining to include newly available data, including consideration of expanded source datasets. The source station precipitation data that were used to form and update the 425 long-term precipitation data series includes the Adjusted Daily Rainfall and Snowfall data from 3346 manual gauge stations (Wang et al., 2017), adjusted precipitation data from 21 Belfort or Fisher-Porter automated gauge stations (see Wang et al., 2023) and from 864 stations of the Community Collaborative Rain, Hail and Snow (CoCoRaHS) network (https://www.cocorahs.org/canada.aspx), together with wind-bias-adjusted precipitation data for the period 2001–2023 from 332 Geonor or Pluvio automated gauge stations (Smith et al., 2022). Each of these supplementary datasets is briefly described below.

As detailed in Wang et al. (2017), the AdjDlyRS dataset (available at https://open.canada.ca/data/en/dataset/d8616c52-a812-44ad-8754-7bcc0d8de305#) adjusted archived station data to correct for known biases. First, conversion of snowfall ruler measurements to their water equivalents was performed using a previously developed snowfall water equivalent adjustment factor map (Mekis & Brown, 2010) instead of the unrealistic 10-to-1 ratio used to calculate total precipitation in the ECCC digital archive. Secondly, corrections were made for trace precipitation amount and for gauge specific biases (such as under-catch and evaporation due to wind effect, as well as gauge wetting loss). Finally, flagged data were adjusted. For example, a daily precipitation amount flagged as a multi-day accumulated amount was distributed to the immediately preceding days of reported precipitation occurrence but zero amount, using neighbour stations' proportions of precipitation amounts over those days. The adjusted data were further subjected to an in-depth quality-control system to identify both erroneous abnormally large values and erroneous zero or near-zero values (Cheng et al., 2024), including the identification and exclusion of long runs of missing values that were miscoded as zero precipitation (see Section 3a below for more details).

The 21 Belfort or Fisher-Porter automated gauge stations, which were also used by Wang et al. (2023), have long data records that are mostly located in the North or in Quebec and thus are an important source of data in areas that are otherwise data sparse.

The CoCoRaHS Canada network began in Manitoba in December 2011 following a massive flood experienced in Manitoba and parts of Saskatchewan. It is "a unique, non-profit, community-based network of volunteers of all ages and backgrounds working together to measure and map precipitation across Canada". According to Rick Fleetwood (personal communication), all volunteers use the standard CoCoRaHS precipitation gauge, which is a professional quality 4-inch gauge very similar to the ECCC Type B gauge and has been tested informally and found to have readings that are very close to the ECCC Type B gauge in side-by-side comparisons. Precipitation reports are submitted once per day, normally between 6 and 9 am local time. We adjusted and quality-controlled precipitation data from 864 CoCoRaHS stations with sufficient data for us to adjust and quality control daily data and to calculate monthly total precipitation amounts. Considering that the CoCoRaHS precipitation gauge is very similar to the ECCC Type B gauge, we adopted the Type B gauge specific adjustment procedure to adjust CoCoRaHS data. A brief note on the adjustment and QC procedures is provided in SM1 of the Supplementary Materials.

Smith et al. (2022) adjusted hourly precipitation data from 397 Geonor or Pluvio automated gauge stations for wind-induced under-catch using the universal transfer function developed by the World Meteorological Organization (WMO) Solid Precipitation Intercomparison Experiment (Nitu et al., 2018). These modern automated gauge data series started in 2001 or later and have a high missing data rate. We were able to quality control and derive monthly precipitation amounts for 332 of these stations.

We then combined the AdjDlyRS manual gauge dataset (3346 stations) with the adjusted Belfort or Fisher-Porter automated gauge data (21 stations), the adjusted CoCoRaHS manual gauge data (864 stations), and the adjusted Geonor or Pluvio automated gauge data (332 stations) to produce version 2 of the Canadian adjusted precipitation dataset, called CanAdjP V2, which includes both daily and monthly precipitation data. All the four source datasets are updated to the end of 2023. Thus, the CanAdjP V2 dataset consists of 4578 stations of varying data record lengths (mostly short records). Figure 1a intercompares the time series of annual count of stations with non-missing monthly data in the CanAdjP V2 and updated AdjDlyRS datasets (annual count multiplied by 12 equals annual count of non-missing data). The addition of data from Geonor or Pluvio automated gauge stations and CoCoRaHS manual gauge stations improves data availability in the period since the mid 2000s, levelling off the sharp decline that started in early 1990s (compare red and green curves in Fig. 1a).

Finally, note that for some stations there can be a delay of months to a few years for the data to go into the ECCC digital archive. Thus, slightly more data are available now than a few years ago, which slightly reduces the number of missing data and enables us to improve station joining for 11 out of the 425 joined data series. The data availability is much improved since 2007 (Fig. 1b). The improvement and extension of data series also make data homogenization slightly easier.

b *ANUSPLIN modelling of data*

ANUSPLIN is a software package (Hutchinson & Xu, 2013) for advanced spatial modelling of climate data at irregularly spaced stations/locations. The model fitting produces thin plate smoothing splines, also called ANUSPLIN surfaces, from which gridded datasets on a user-desired grid can be derived. MacDonald et al. (2021) fitted ANUSPLIN models to the AdjDlyRS dataset (Wang et al., 2017), producing the ANUSPLIN surfaces and gridded datasets of adjusted precipitation the (ANUSPLIN-gridded Adjusted Precipitation (ANUSPLIN-AdjP) datasets for Canada is available at https://open.canada.ca/data/en/dataset/779ea77a-0ad1-42f2-853e-833e1cbb9a13). These surfaces provided ANUSPLIN estimates of monthly precipitation to infill gaps in the 425 long-term data series that formed the basis for CanHomP adjusted and homogenized monthly mean precipitation dataset produced by Wang et al. (2023). The CanAdjP V2 dataset described above was used as input to run ANUSPLIN modelling in the same setting as MacDonald et al. (2021). This was done for both monthly and daily time scales, producing the monthly and daily ANUSPLIN surfaces, as well as ANUSPLIN-gridded adjusted monthly and daily precipitation datasets (ANUSPLIN-adjP mlyV2 and dlyV2). Data gaps in

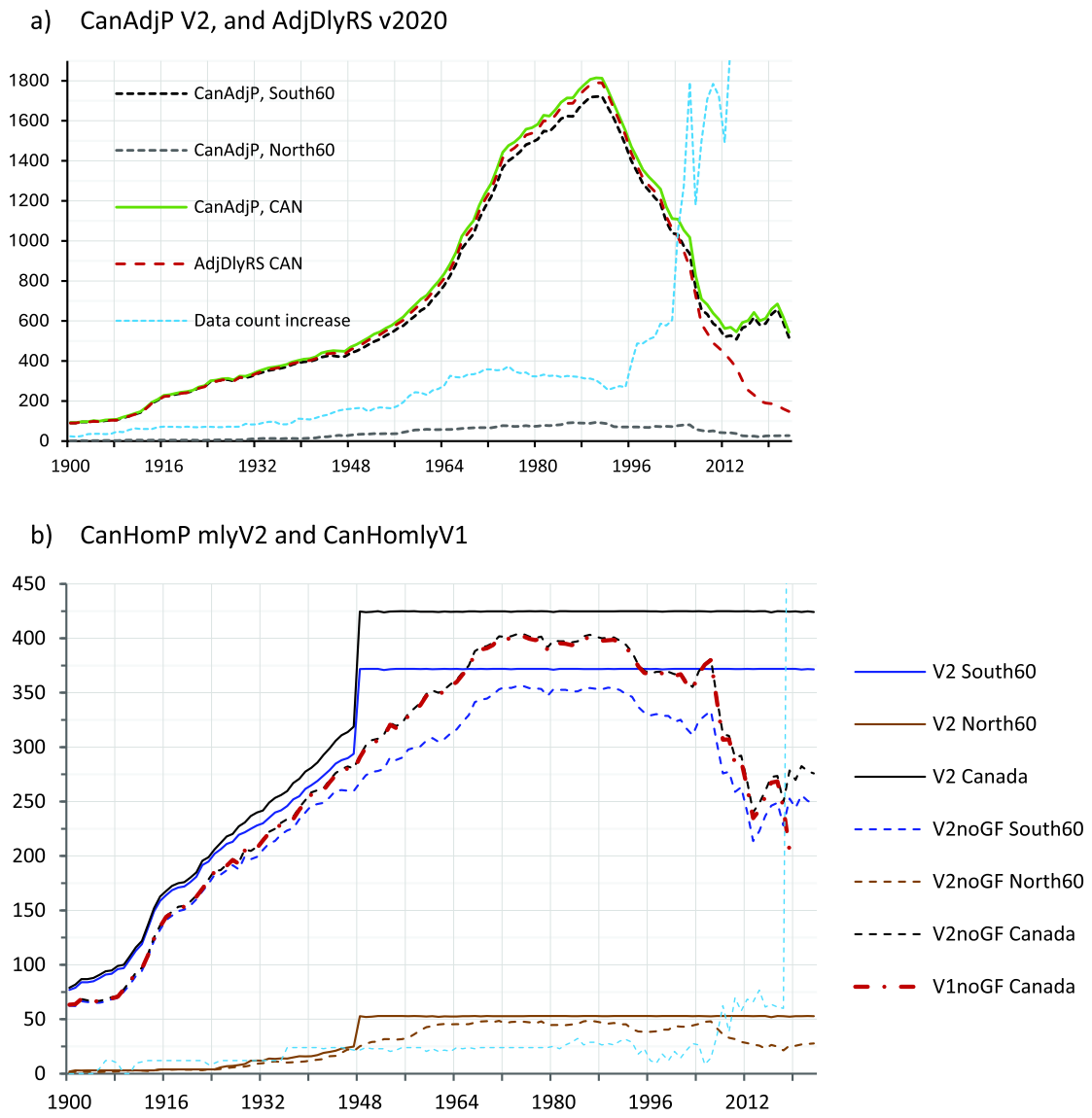

Fig. 1 Time series of annual count of stations with non-missing monthly precipitation data in the CanHomP mlyV2, CanAdjP V2, and AdjDlyRS (updated to 2023) datasets in the indicated regions. Here, the annual count of stations was estimated as the corresponding annual counts of non-missing monthly data (i.e. data count) divided by 12. V1noGF and V2noGF refers to the CanHoPmlyV1 and CanHomP V2 station data without the data gaps infilling, respectively. The data count increases are (a) from v2020 to V2, (b) from V1noGF to V2noGF.

the 425 CanHomP stations were infilled with corresponding values from ANUSPLIN surfaces, with both endpoints of the segment of infilled values being recorded as documented changepoints for homogeneity testing. The gap-infilled data series were then subject to homogeneity testing and homogenization (Wang et al., 2023). Figure 2 shows the flowchart of the homogenized data production procedures we carried out in this study.

c *Reanalysis precipitation data*

As in Wang et al. (2023), the ensemble-mean monthly precipitation data taken from the United States National Oceanic and Atmospheric Administration Twentieth Century Reanalysis version 3, 20CRv3 (Slivinski et al., 2019), were used as reference to help identify artificial changepoints but were not used in homogenization of the station data series. 20CRv3 provides an 80-member ensemble of moderate resolution (~75 km) analyses of the full atmospheric state for 1836 to 2015, by assimilating only sea surface temperature and atmospheric surface pressure observations. OCADA is the Over-Centennial Atmospheric Data Assimilation reanalysis dataset produced by Japanese institutions. It is like 20CRv3 but uses a Japanese atmospheric model to provide moderate resolution (~60 km) analyses of the full atmospheric state (Ishii et al., 2024).

To assess the effects of changing data availability over time on estimates of precipitation trends, we need a gridded dataset that spans the CanGridP V2 data period (1900–2023). For this purpose, we use ERA5 for the 1948–2023 period along with

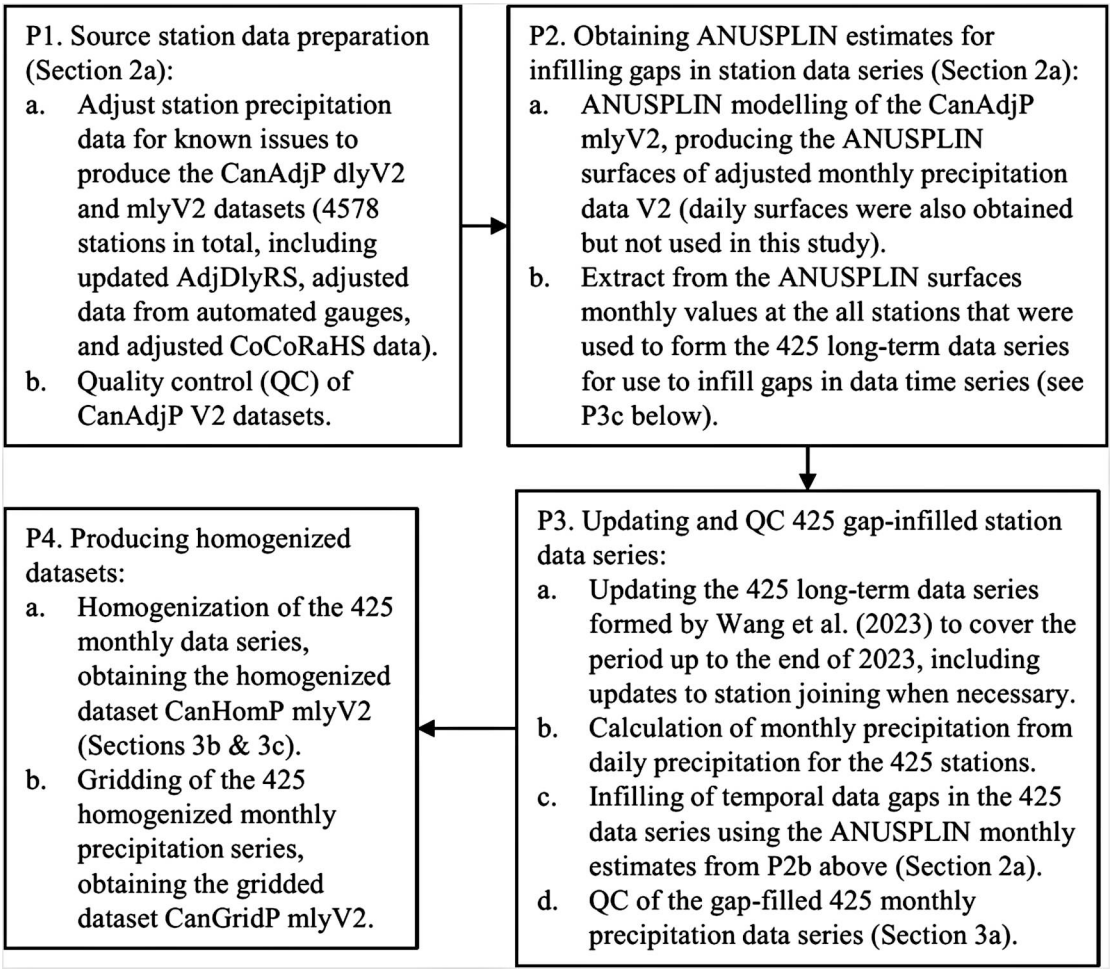

Fig. 2 The flow chart of the homogenized data production procedures.

ensemble-means of the 20CRv3 and OCADA reanalysis ensembles for the 1900–2015 period. ERA5 is the fifth generation ECMWF reanalysis for the global climate and weather, produced by assimilating an extensive archive of historical in situ and satellite observations (Hersbach et al., 2020). It provides high resolution (~31 km) analyses of the full atmospheric state for 1940 to the present. Due to data inhomogeneity concerns, we used ERA5 data from 1948 to 2023.

d *Canadian homogenized temperature data*

Precipitation scaling rate is the percentage of increase per 1°C of warming in the region in question, which provides a measure of the sensitivity of the average amount of precipitation to a change in average temperature, as well as a benchmark for comparing climate models. To assess precipitation scaling rates, we also used version 3.1 of the gridded Canadian homogenized temperature data, CanGridT mlyV3.1, which is an updated and gridded version of the third generation of Canadian homogenized surface air temperature station data developed by Vincent et al. (2020). More details about the CanGridT mlyV3.1 and its representativeness of warming trend in Canada are provided in SM2 of the Supplementary Materials.

3 Quality control and homogenization method improvements

a *Additional quality control procedure*

As when producing CanHoPmlyV1, we also used the quality control (QC) system of Cheng et al. (2024) to identify erroneous abnormally large and erroneous small (zero or near-zero) values. This basically automatic QC system does not work well, however, when few neighbour observations are available for comparison to help distinguish erroneous values from valid ones. Thus, we also carried out a visualization-aided manual QC of the 425 data series to identify mis-recorded missing values (see next paragraph for details). These are zero or near zero monthly precipitation amounts that arose from missing daily observations being mistakenly recorded in the archive as zero precipitation amounts for all or most days in the month. Near-zero monthly precipitation amounts (mostly 0.1–0.3 mm) usually result from corrections for trace precipitation (i.e. adding a small trace precipitation

amount to a day of recorded zero precipitation amount with a trace precipitation occurrence flag) that were made when producing the AdjDlyRS dataset (Wang et al., 2017). In a few cases, these amounts also resulted from the occurrence of a few valid daily observations in a month of mostly mis-recorded missing observations. Such cases usually occur immediately before or after a data gap (a period of missing observations). As in Cheng et al. (2024), the manual QC for identifying erroneous small monthly precipitation amounts is based on the log-transformed monthly precipitation data series.

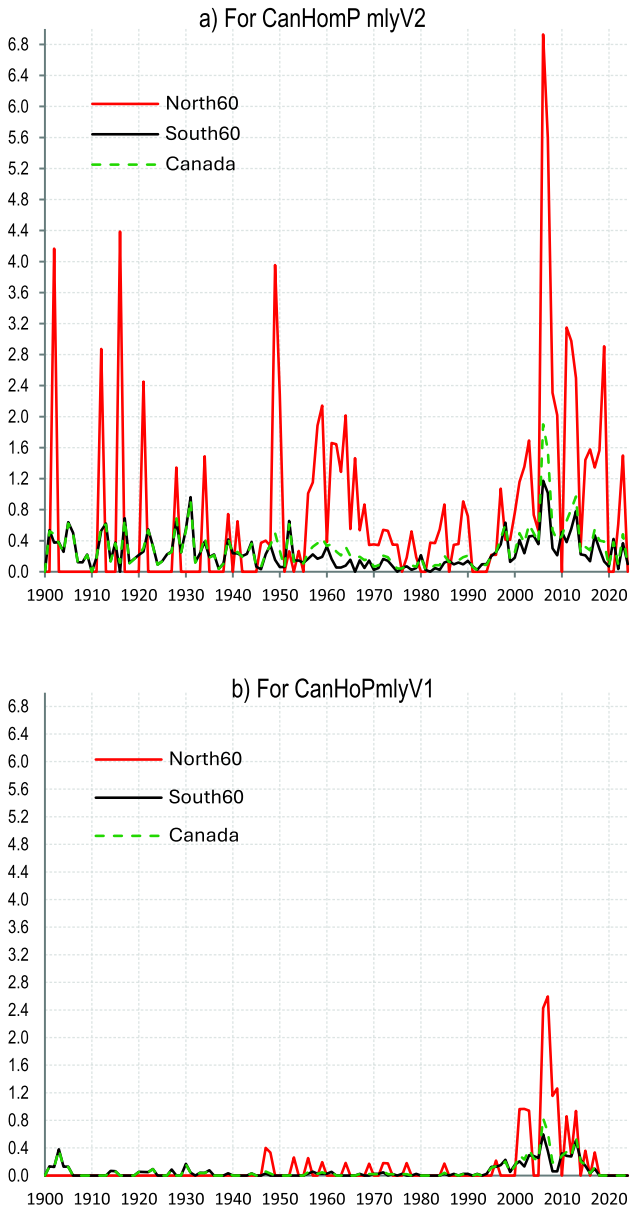

Fig. 3 Annual rates (%) of erroneous precipitation data in the indicated regions north and south of 60°N latitude (North60 and South60) and in whole Canada, identified and excluded for producing the (a) CanHomP mlyV2 and (b) CanHoPmlyV1 datasets.

Our QC procedure identified 1244 erroneous values in the updated 425 station data series. Most of these values are zero or near zero monthly precipitation amounts that correspond to mis-recorded missing values that are clearly visible outliers in the de-seasonalized log-transformed series. These usually occurred in only one period with no similar values outside that period (a problem unique to that period of observations) or are adjacent to a month of partial or fully missing observations. They are usually found in winter when data were not reported due to the use of a gauge that cannot measure solid precipitation (e.g. unheated tipping bucket rain gauges). For some stations, these outliers (zero or near-zero values) occur in the same winter month (or months) for a few years in sequence (a pattern of a sort of "vacation period"). The ANUSPLIN estimates for these months are substantially different from the zero or near-zero values and are much more in line with the other values in the data series, thus helping us to identify erroneous values. Most of these erroneous values were replaced with the corresponding ANUSPLIN estimates. There are a few cases in data sparse periods or areas (mostly before 1900) for which good ANUSPLIN estimates are not available, in which case we decided not to trust the outlier log-transformed value and set it to missing without infilling the data gap.

The QC procedure applied to produce the previous CanHoPmlyV1 dataset failed to identify hundreds of mis-recorded missing values in northern Canada throughout the whole data record period, and in southern Canada in the pre-1970 period. As shown in Fig. 3, the error rates are lowest in the period from 1970 to 1995 (especially in southern Canada), increased in the late 1990s to around 2015 (which is associated with an increase in automated gauge data), while data from northern stations (north of 60°N) have much higher error rates than those from southern stations.

For example, visualization-aided QC of the joined data series for the Ivvavik National Park (2100660) station in northern coast of Yukon identified eight erroneous zero values and 13 erroneous small monthly total precipitation values (0.1 to 0.3 mm) in the period before April 1973. These erroneous zero or near-zero monthly precipitation amounts were left in the CanHoPmlyV1data series, but are set to missing and mostly infilled with ANUSPLIN data in CanHoP mlyV2. As shown in Fig. 4, the erroneous values (red circles in panel a) caused the data segment with the erroneous values to have a different variance than the rest of the data series. After replacing these erroneous values with the corresponding ANUSPLIN estimates, the data series is more homogenous in variance (Fig. 4c). This made a difference in detecting changepoints and in estimating adjustment amounts to homogenize the data series, as shown in panels b, d. Gridding such erroneous zero or near zero monthly precipitation amounts can affect large areas when the station density is low, such as in the pre-1970 period or in northern Canada throughout the data record period, leading to lower regional mean precipitation amounts in the pre-1970 period. This is one of the reasons for the apparent rapid rise in the

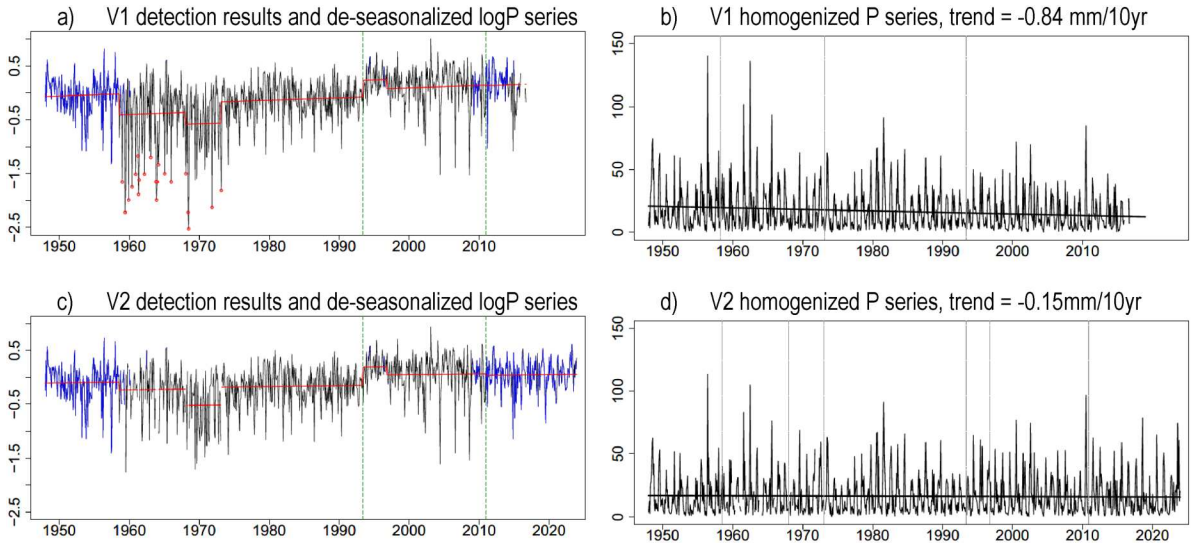

Fig. 4 Comparison of V2 and V1 detection and homogenization results for the Ivvavik National Park station (ID: 2100660). The logP series is log(P+0.1), with precipitation (P) in mm. The V1 data series contains 20 mis-recorded missing values (0–0.3 mm) in the period before April 1973 (red circles in c) that were identified and set to missing in V2. The ANUSPLIN estimates that were used to infill data gaps are shown in blue. The vertical green dashed lines (a, c) mark station joining, and the vertical grey lines (b, d) mark the changepoints detected and adjusted.

regional mean precipitation amount in the 1960s (see the dashed red line in Fig. 5). The V1 data were found to have a significant changepoint at the end of October 1963 in the regional mean series for southern Canada, where this is no longer apparent in the V2 data. The 30-year running means of anomalies of the regional mean annual precipitation in the V2 data evolves as nearly a straight line (black solid line in Fig. 5a), although the regional mean series for northern Canada and whole Canada were found to have a significant changepoint at the end of November 1948 (primarily due to the data availability increase around this time; see Fig. 1b, orange and black solid lines). These are considered in trend analysis (see Section 5).

b *Improved changepoint detection procedure*

Changepoints are discontinuities in a climate data time series that are caused by non-climatic factors, such as changes in observing locations/environment, instrument, etc. These can affect estimates of the mean or variance or the whole distribution of the data and must be removed from the data series through data homogenization so that the data series can better present the true climate and its changes. Homogenization includes two steps, changepoint identification and subsequent data adjustment to remove the identified discontinuities (shifts).

Several statistical tests have been developed for changepoint detection. In particular, the RHtestsV4 software package (Wang & Feng, 2013) includes functions that use regular t- or F-tests for detecting changepoints with known causes that are documented in metadata (type-0 changepoints) and functions that use penalized maximal t- or F-tests (Wang, 2008a, 2008b; Wang et al., 2007) for detecting changepoints of unknown causes (type-1 changepoints). Both account for autocorrelation of the data series (Wang, 2008a). Using the RHtestsV4 functions, Wang et al. (2023) developed a semi-automatic comprehensive procedure of multiple tests with and without using reference series for monthly precipitation data homogenization. It used up to six reference series, including the 20CRv3 ensemble-mean monthly precipitation series for the grid point closest to the station, the ANUSPLIN estimates of monthly precipitation for the station, and up to four best significantly-correlated (at 5% level) data series from neighbouring stations located within a 200 km radius of the station being homogenized (where correlations are determined based on times series of first differences).

We used the semi-automatic procedure with three small modifications. One is that we retained all potential type-0 changepoints of station-joining until all other significant changepoints were identified, then re-assessed the statistical significance of these changepoints in the presence of the other identified changepoints. At the early testing stage, the changepoints associated with station-joining were retained for further testing if they are more likely to be significant than not (using 25% level of significance). At the final manual investigation, changepoints of station-joining were retained for adjustment if they are significant at 10% level (except cases associated with a variance change), considering that these have a reliable cause and could bias the trend estimate for the series to make it inconsistent with its surrounding stations even when the mean-shift it caused is of low statistical significance as noticed in Wang et al. (2023). The second modification is that we retained changepoints with visible variance changes even if the associated change in the mean is not statistically significant, which allows us to adjust for variance inhomogeneity (mostly associated with station joining or

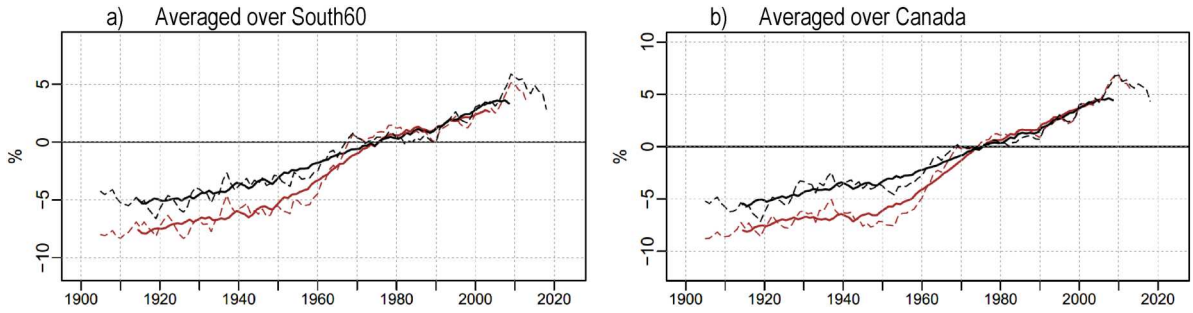

Fig. 5 Comparison of the 11-year (dashed lines) and 30-year (solid lines) running means of anomalies of the spatially averaged annual total precipitation amount expressed relative to its climatological mean amount for the 1961–1990 baseline period (baseline value). Anomalies of spatial means (averaged over Canadian land mass) and corresponding baseline values are obtained from CanGridP mlyV2 (black lines) and CanGridP mlyV1 (red lines).

segments of ANUSPLIN estimates). Other than these special cases, we also set the significance level for detecting changepoints to 1% to avoid over-adjusments to the data as was done in Wang et al. (2023). The third modification is that we also tested and visually investigated the untransformed data series in addition to the log-tranformed data series, while only the latter was tested and visually investigated for producing CanHoPmlyV1. This is very important due to the unique characteristics of precipitation data (non-negative and skewed data). The modified changepoint detection procedure is detailed in SM3 of the Supplementary Materials.

Importantly, the metadata used to produce CanHomP mlyV2 were much more complete than for CanHoPmlyV1. In particular, we found that the record of CanHoPmlyV1 station joining times, which was manually recorded in metadata at the time, was incomplete. We therefore ensured that CanHomP mlyV2 was accompanied by a complete record of station joining times. Such improved metadata, along with the new procedure for testing changepoints of station joining, result in improved changepoint detection results and thus improved homogenized dataset, as shown in Fig. 5 and discussed in Section 6.

The current changepoint detection methods are limited to detecting sudden changes in the mean and do not deal with non-climatic gradual changes that may also arise from gradual changes in the environment of the observing site that may affect precipitation observations (such as changes in near surface winds due to vegetation growth and/or infrastructure development, which affect gauge collection efficiency). However, our careful visual inspection of the 425 precipitation data series did not find any noticeable gradual changes.

c *Improved adjustments to eliminate data inhomogeneity*

Having finalized the list of changepoints identified in each of the 425 data series, we used a modified version of the quantile matching (QM) method in the RHtestsV4 package to adjust the data series in question to obtain the homogenized series. Unlike in Wang et al. (2023), which made adjustments to the log-transformed data series, adjustments were made to the untransformed precipitation data series in this study. This is necessary, because we noticed that using log-transformed data series to estimate and apply the adjustments could introduce artificial variance changes in the adjusted precipitation data series. Note that we kept the observed amount unchanged in the very rare instances where an adjustment would have produced an unphysical negative value. The second modification is to allow segments that are too short for QM adjustments to be feasible to be combined with neighbouring segments by first making mean adjustments after which the remaining changepoints are addressed using the QM method. Consistent with Wang et al. (2023), reference series were not used when making the adjustments in this study. They showed that when station density is too low to find good reference stations, adjustments to monthly precipitation without a reference are better than those with a reference for some stations, while they are very similar for the other stations. However, this might not be applicable for precipitation data of much higher station density or other variables of much higher spatial coherence (such as temperature).

Note that the QM method adjusts the whole distribution of the data in one segment to match another (Wang et al., 2010; Wang et al., 2023). Thus, distribution changes (including variance changes) at the identified changepoints are also homogenized. For example, for the Port Alberni Airport station in British Columbia (BC), there is an obvious variance change at the time of station joining in the end of December 1965 (Fig. 6a), which no longer exists in the homogenized data series (Fig. 6c).

4 Characteristics and effects of data inhomogeneity

We identified 1125 artificial changepoints in 360 out of the 425 long-term precipitation data series, including 891 type-0 and 234 type-1 changepoints. The remaining 65 data series were found to be homogenous. Figure 7 shows the annual series of percentage of stations (i.e. data series) with at least one changepoint of type-0 (blue line), type-1 (red line), and either type (black line). Type-1 changepoint relative frequency (Fig. 7, red line) decreases over time, with two notable drops around 1955 and 1975, which are due to improvement in metadata collection and more missing data in the recent decades (missing data information was used as

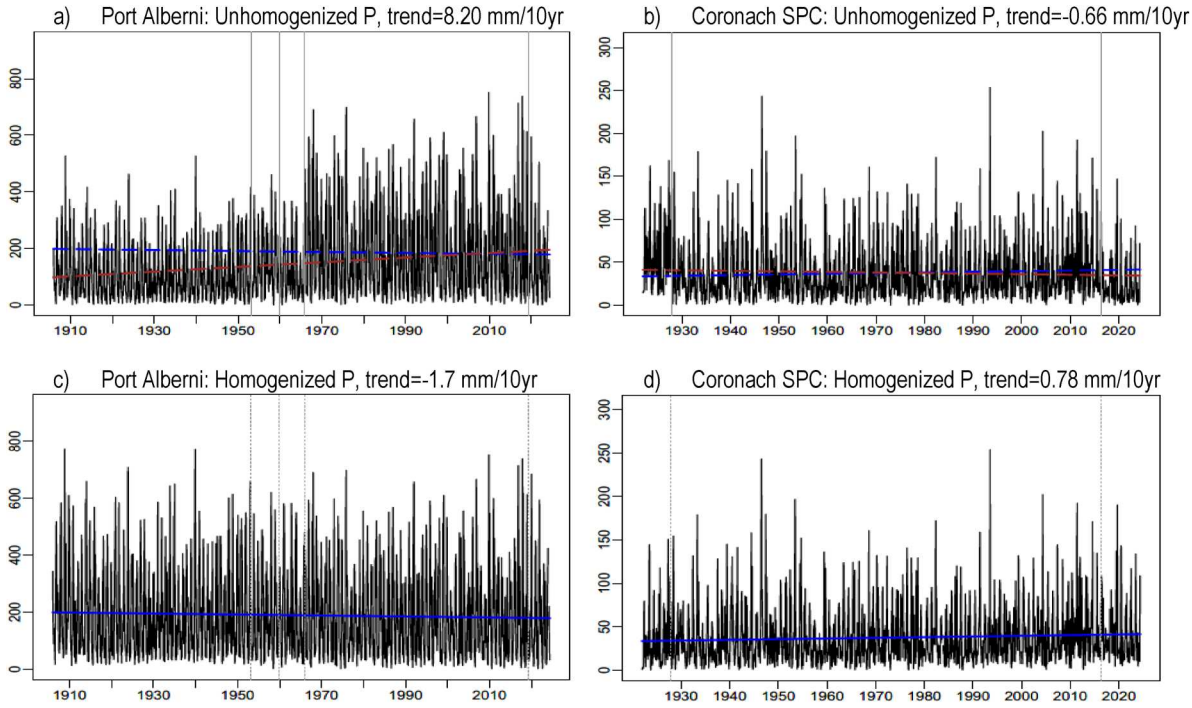

Fig. 6 The unhomogenized and homogenized precipitation (P) data series for Port Alberni Airport (AUT) (ID: 1036B06) and Coronach SPC (ID: 40318MN) station. The thin vertical lines mark the changepoints identified and adjusted. The unhomogenized P trend is shown in red, and homogenized P trend, in blue.

metadata in this study; see SM3). Type-0 changepoint relative frequency is the lowest in the period from the late 1960s to around year 2000 (mostly below 2%) but becomes very high in the recent two decades, and is also higher in the early period, especially around 1930. The high percentages in the last two decades are due to station automation and more missing observations in the automated gauge data records, and the peak around 1930 was due to relatively more data gaps in this period according to Wang et al. (2023).

Compared to the V1 results, the biggest increase is in the number of type-0 changepoints, which arose from better availability of metadata (e.g. more complete metadata on station joining) and extension of the 425 data series from September 2019 to the end of 2023, a period of very high percentages of type-0 changepoints (Fig. 7, blue line). Among these type-0 changepoints, 27.6% are due to station-joining, 17.4% are due to changes in gauge type and/or observing frequency, and 55.0% are due to other changes accompanied with a data gap. Most of the inhomogeneous series are multi-changepoint (3 or more) series; only 75 of these are single-changepoint series, and 91 are two-changepoint series.

Wang et al. (2023) presented the effects of data inhomogeneities on trend estimates with examples and comparison of trend maps from unhomogenized and homogenized data series. We show two examples of the effects on trend estimates for the individual station series in Fig. 6: a small decrease at Port Alberni Airport (BC) was biased to a large increase, and a small increase at Coronach SPC (Saskatchewan) station was biased to a small decrease. Further, we present the map of trends estimated from the homogenized and unhomogenized data series for the 425 locations in Fig. 8. The homogenized dataset shows better spatial consistency of trends, especially in Atlantic Canada and BC.

5 Precipitation trends

We now present Canada's historical precipitation trends as estimated using the CanGridP mlyV2 dataset, a gridded version of the CanHomP mlyV2 dataset produced in this study. Like in Wang et al. (2023), the gridding was done using a kriging-based algorithm that grids the normal values and anomalies relative to the normal values separately (Abbasnezhadi & Wang, 2024), and trends were estimated using the method of Wang and Swail (2001), a variant of the Sen's non-parametric slope estimator and Mann-Kendall trend significance test that accounts for autocorrelation in the data series. Since the regional mean series was found to be homogenous since 1900 for southern Canada, and since December 1948 for northern Canada and whole Canada (Section 3a), we will focus on the periods 1900–2023 and 1949–2023. First, we assess the representativeness of CanGridP mlyV2 for Canadian precipitation trends. To this end, we subsampled a reanalysis dataset (20CRv3 and OCADA for 1900–2015, ERA5 for 1949–2023) to produce gridded data that mimic CanGridP mlyV2 in terms of the set of station locations and the data availability at these locations. We compared trends estimated from this subsampled

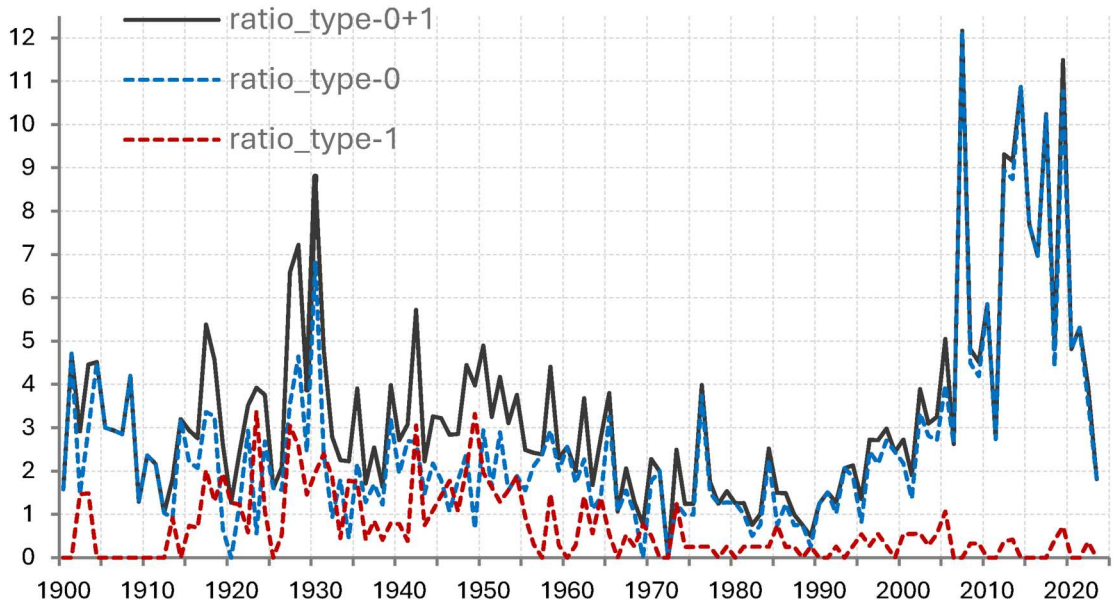

Fig. 7 Time series of percentage of stations with at least one changepoint of the indicated type(s) in the year (horizontal axis).

reanalysis dataset with the benchmark trends estimated from the complete reanalysis dataset. The results (see supplementary Fig. S1) show that the CanHomP stations network with gap infilling well represents trends in the region south of 60°N (South60) for the periods 1949–2023 and 1916–2015 (there is no reanalysis data for assessing the 1916–2023 trend). Both the trend and its confidence range are within the confidence range of the corresponding benchmark trend, although the 1949–2023 trend is slightly overestimated, and the 1916–2015 trend, slightly underestimated. Larger underestimate is seen for the 1900–2015 trend. Results for the region north of 60°N (North60) are similar in character, but consistency is lower for the century-long periods 1916–2015 and 1900–2015, with the 1900–2015 trend estimate falling outside the confidence range of the corresponding benchmark trend. Thus, hereafter we will focus on trends since 1916 for southern Canada and since 1949 for northern Canada and whole Canada.

The years 1916 and 1949 were chosen because the 11-year running mean series of anomalies of regional mean precipitation from the subsampled dataset well overlap the corresponding benchmark series (not shown). These coincide with the considerable increase in the amount of data around these years in southern and northern Canada respectively (Fig. 1b).

a *Annual precipitation trends*

As shown in Fig. 9, annual total precipitation trends indicate significant increases in most areas from southern Nunavut to the Canadian Arctic Archipelago, from Yukon to northern BC and southern Northwest Territories (NWT), from Labrador to northeastern Quebec, and along the St. Lawrence River basin. This is accompanied with a significant decrease in small areas in northern NWT, southern Alberta, and eastern Canada. For the 1949–2023 period, 51.8% of the gridpoints were found to have a significant trend; 82.5% of the gridpoints have a positive trend, with the largest relative increase being seen in Nunavut, while the largest increase in physical unit (mm) is seen in southeastern Canada and southern BC (Fig. 9a,b). For the century-long period from 1916 to 2023, 61.0% of the gridpoints in Canada's South was found to have a significant increase, with 86.9% of the gridpoints having a positive trend.

For the eight regions used in Canada's Changing Climate Report 2019 (Bush & Flato, 2019; Zhang et al., 2019), Table 1 presents linear trends in the regional mean annual total precipitation series, along with relative trends that are expressed in percentage of the 1961–1990 mean value of the data series in question. Over the period 1949–2023, regional mean annual precipitation is estimated to have increased at a rate of 1.31% per decade for Canada, 2.55% and 1.01% per decade for Canada' North and South, respectively. Except the Prairies and Ontario where precipitation increase is not statistically significant (at 5% level), all other regions have experienced a statistically significant increase in the regional mean annual precipitation amount. Over the century-long period 1916–2023, precipitation in Canada's South also increased at a rate of 1.00% per decade. Regional mean annual precipitation trends are also different for different regions in southern Canada, with the highest relative increase in the Atlantic region, followed by BC, for both periods 1949–2023 and 1916–2023 (Table 1). The 1949–2023 trends in provincial/territorial mean annual precipitation series are provided in supplementary Table S2.

Canada's 10 highest estimated annual precipitation amounts in the period of 1949–2023 have occurred since

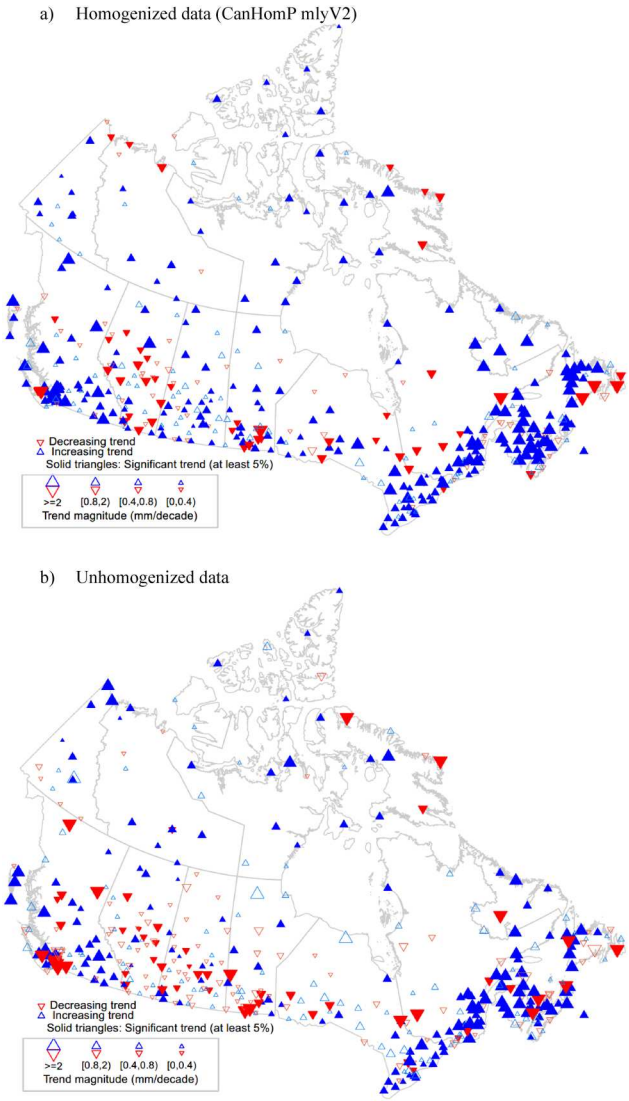

Fig. 8 Trends over the data records periods in the homogenized and unhomogenized station data series (homogenized data series includes quality control and data gap infilling).

1996 (Fig. 10a,b). The best estimate of increase between 1949 and 2023 is 9.7% for Canada as a whole, 18.9% for Canada' North, and 7.5% for Canada's South. Over the period between 1916 and 2023, mean annual precipitation in Canada's South has increased 10.7%. After around 1960, CanGridP mlyV2 is in good agreement with ERA5 in terms of changes in annual precipitation averaged over Canada (Fig. 10).

b *Seasonal precipitation trends*

As shown in Fig. 11, Canada's precipitation trends have notable seasonality. The pattern of precipitation change varies from season to season. Winter precipitation has decreased significantly in central-south Canada, while it has increased significantly in most areas in northern Canada, especially from southern Nunavut to the Arctic Archipelago and from northern Yukon to southern NWT, and part of northern Quebec. Winter and spring precipitation share a similar pattern of changes in northern Canada but show substantially different changes in southern Canada, where we see dominantly negative trends in winter but dominantly positive trends in spring. In southern Canada, spring precipitation increase is most prominent in BC and is also seen in some areas in the region from central Manitoba to the St. Lawrence River basin, while the increases in northern Quebec are more extensive in spring than in winter. Summer precipitation changes are characterized by increases in the eastern Arctic and in a zonal band around 60°N across the country, accompanied with small areas of decreases in northern NWT coasts, southern Vancouver Island, and northern Ontario to central Quebec. Spring precipitation also increased along the St. Lawrence River basin. Autumn precipitation trend pattern is like that of spring but with smaller relative changes that are also significant in smaller areas except in southeastern Canada (Fig. 11b,d).

The regional mean trends also show some seasonality, and the seasonality in Canada's North is different from that in Canada's South (Table 1). In Canada's North, the largest relative increase among the four seasons is seen in spring, with slightly smaller relative increase in winter, and the smallest relative increase in autumn. In Canada's South, winter precipitation has an insignificant decrease, although precipitation also has the largest relative increase in spring, with slightly smaller relative increase in autumn, and the smallest relative increase in summer. Note that all other increases mentioned here are statistically significant.

c *Precipitation scaling rates*

Using the new datasets CanGridP mlyV2 and CanGridT mlyV3.1 (see Section 2d and SM2), Canada's annual precipitation scaling rate is estimated to be 2.6% per 1°C of warming for the period 1970–2023, and 4.9% for the period 1949–2023. The scaling rate is higher in Canada's North than in Canada's South (5.6% versus 2.7% for the period 1970–2023, and 6.9% versus 5.1% for 1949–2023). The higher scaling rates in Canada's North are generally consistent with our understanding of how the climate system will alter and redistribute precipitation due to human influence on the climate (Lee et al., 2021). For the century-long period 1916–2023, the estimated scaling rate is 6.7% for Canada's South, but no reliable estimate can be obtained for Canada's North. Note that these scaling rate estimates can only be interpreted cautiously as they are based only on best estimates of precipitation increases and warming rates, both of which have some degree of uncertainty.

The new datasets yield nevertheless estimates of scaling rates (all are under 7% per 1°C of warming) that are more in line with physically based expectations than those estimated from the previous CanGRD and CanGridP mlyV1 datasets (see supplementary Table S1), which both exhibited much higher scaling rates.

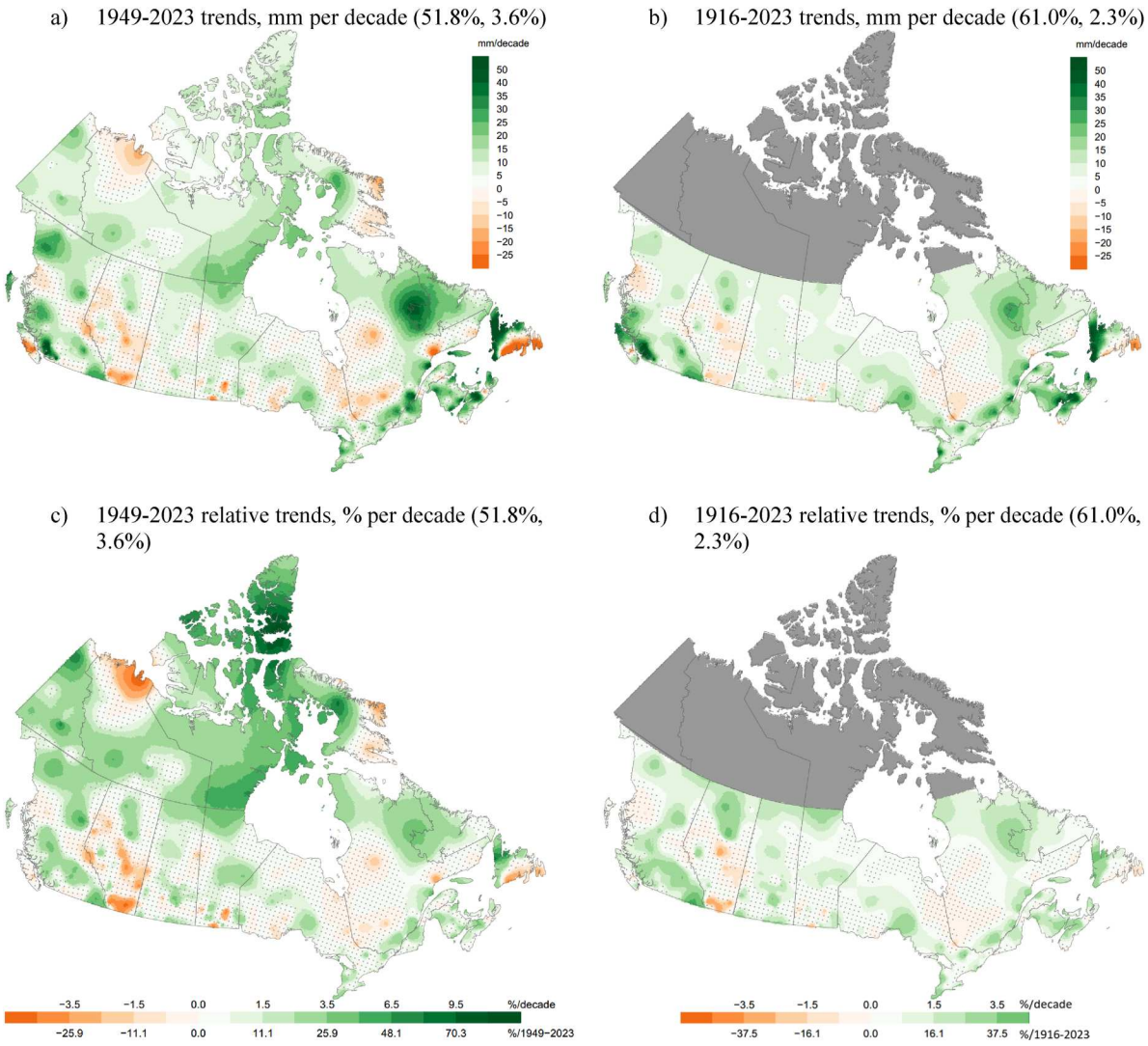

Fig. 9 Maps of trends in annual total precipitation over the indicated periods. The relative trends are the trends expressed as percentages of the corresponding mean over the 1961–1990 period. Areas with statistically insignificant trends are dotted (significance was determined via a two-sided test at 5% level). The percentage given in the panel title is the percentage of grid points with significant (positive, negative) trends, indicating field significance or lack of it.

6 Summary and discussion

We have reported the development of the second version of Canadian homogenized monthly precipitation dataset, CanHomP mlyV2, and provide updated estimates of how precipitation in Canada has changed using a gridded version of that dataset, with an assessment of representativeness of trends in the gridded dataset.

CanHomP mlyV2 was produced using improved station data and metadata (Section 2), as well as an improved data homogenization procedure that uses multiple homogeneity tests (Section 3). As in Wang et al. (2023), the 425 homogenized station data series are gap infilled, with only a very small number of missing data remaining in a few data series (for which reliable estimated infill values are not available). The new homogenized station dataset shows better spatial consistency of trends than does the unhomogenized dataset and was gridded to the 10-km grid as in Wang et al. (2023), producing the CanGridP mlyV2 gridded dataset.

Further, we have used CanGridP mlyV2 to characterize historical precipitation trends in Canada. The new trend estimates are smaller in magnitude and much more in line with physically based expectations than those reported in Vincent et al. (2015) and Zhang et al. (2000). They also show notable improvements over the CanGridP mlyV1 based estimates, with the rapid rise in the 1960s, which appears to have been primarily due to widespread miscoding of missing values as zero in the earlier part of the record, being substantially diminished (Fig. 5). In addition, we have performed a preliminary assessment of the potential impact of sampling bias in trend estimates due to the changing availability of data over time and found that changes in data availability likely do not significantly affect trends in regional mean precipitation when calculated

TABLE 1. Trends in the regional mean series of seasonal or annual total precipitation over the indicated periods, as estimated from the CanGridP mlyV2 dataset. The 95% confidence interval of trend is shown in parenthesis. Insignificant trends are shown in italic. The regions are as defined in Canada's Changing Climate Report (Bush & Flato, 2019). Canada's South includes British Columbia, the Prairie provinces, Ontario, Quebec, and Atlantic Canada.

Period	Region	Annual	Winter	Spring	Summer	Autumn
(a) Trends in physical units (mm/decade)						
1949–2023	Canada	8.26 (5.92 to 10.41)	*0.44 (−0.77 to 1.53)*	2.89 (1.35 to 4.42)	2.28 (0.93 to 3.57)	2.63 (1.08 to 3.94)
	Canada's North	8.39 (3.81 to 13.16)	2.16 (1.31 to 3.12)	2.54 (1.15 to 4.08)	2.64 (1.02 to 3.89)	1.34 (0.28 to 2.41)
	Canada's South	8.09 (2.67 to 12.7)	*−0.46 (−2.07 to 1.11)*	2.98 (1.47 to 4.45)	1.9 (0.34 to 3.75)	3.69 (1.35 to 5.75)
	British Columbia	10.99 (1.96 to 18.37)	*−1.18 (−6.18 to 3.17)*	5.01 (1.74 to 8.16)	*2.31 (−2.00 to 6.64)*	5.14 (1.11 to 8.97)
	Prairie Region	*3.36 (−0.53 to 7.51)*	*−0.46 (−1.51 to 0.57)*	*1.36 (−0.58 to 3.28)*	*1.70 (−1.01 to 4.83)*	*0.89 (−1.77 to 3.33)*
	Ontario	*4.89 (−1.84 to 11.15)*	*−0.17 (−3.15 to 2.84)*	*2.48 (−0.16 to 5.05)*	*1.23 (−2.19 to 4.78)*	*2.52 (−1.23 to 5.70)*
	Quebec	8.08 (1.74 to 13.98)	*−0.48 (−3.12 to 2.06)*	3.65 (1.35 to 5.98)	*1.01 (−1.95 to 3.94)*	4.35 (1.07 to 7.63)
	Atlantic Region	18.39 (11.15 to 24.58)	*2.37 (−1.96 to 6.51)*	3.70 (0.02 to 7.80)	5.64 (2.62 to 9.30)	7.81 (2.88 to 12.65)
1916–2023	Canada's South	8.00 (4.19 to 11.74)	*1.01 (−0.02 to 1.99)*	1.50 (0.72 to 2.37)	2.33 (1.34 to 3.38)	3.13 (1.63 to 4.63)
1970–2023	Canada	6.14 (1.05 to 11.26)	*0.31 (−1.66 to 2.05)*	*1.78 (−0.08 to 3.44)*	2.78 (0.83 to 4.96)	*1.95 (−0.79 to 4.28)*
(b) Regional mean relative trends (%/decade) as derived by expressing the trends in Table 1a in percentage of the 1961–1990 mean of the corresponding data series.						
1949–2023	Canada	1.31 (0.94 to 1.66)	*0.34 (−0.59 to 1.17)*	2.38 (1.11 to 3.64)	1.15 (0.47 to 1.8)	1.48 (0.61 to 2.22)
	Canada's North	2.55 (1.16 to 3.99)	4.23 (2.58 to 6.12)	4.53 (2.05 to 7.27)	2.21 (0.85 to 3.26)	1.30 (0.27 to 2.34)
	Canada's South	1.01 (0.33 to 1.59)	*−0.26 (−1.18 to 0.63)*	1.87 (0.92 to 2.79)	0.78 (0.14 to 1.54)	1.67 (0.61 to 2.61)
	British Columbia	1.3 (0.23 to 2.17)	*−0.47 (−2.46 to 1.26)*	3.29 (1.14 to 5.36)	*1.28 (−1.11 to 3.67)*	1.99 (0.43 to 3.47)
	Prairie Region	*0.65 (−0.10 to 1.46)*	*−0.59 (−1.92 to 0.72)*	*1.34 (−0.57 to 3.24)*	*0.79 (−0.47 to 2.27)*	*0.74 (−1.47 to 2.76)*
	Ontario	*0.58 (−0.22 to 1.33)*	*−0.10 (−1.96 to 1.77)*	*1.48 (−0.09 to 3.02)*	*0.45 (−0.81 to 1.76)*	*1.05 (−0.51 to 2.38)*
	Quebec	0.85 (0.18 to 1.47)	*−0.24 (−1.56 to 1.02)*	1.93 (0.71 to 3.16)	*0.36 (−0.69 to 1.39)*	1.57 (0.39 to 2.76)
	Atlantic Region	1.48 (0.90 to 1.98)	*0.69 (−0.57 to 1.9)*	1.35 (0.01 to 2.83)	1.88 (0.87 to 3.1)	2.44 (0.90 to 3.95)
1916–2023	Canada's South	1.00 (0.52 to 1.47)	*0.57 (−0.01 to 1.13)*	0.94 (0.45 to 1.49)	0.96 (0.55 to 1.38)	1.42 (0.74 to 2.1)
1970–2023	Canada	0.98 (0.17 to 1.79)	*0.24 (−1.28 to 1.58)*	*1.46 (−0.06 to 2.83)*	1.40 (0.42 to 2.5)	*1.10 (−0.44 to 2.41)*

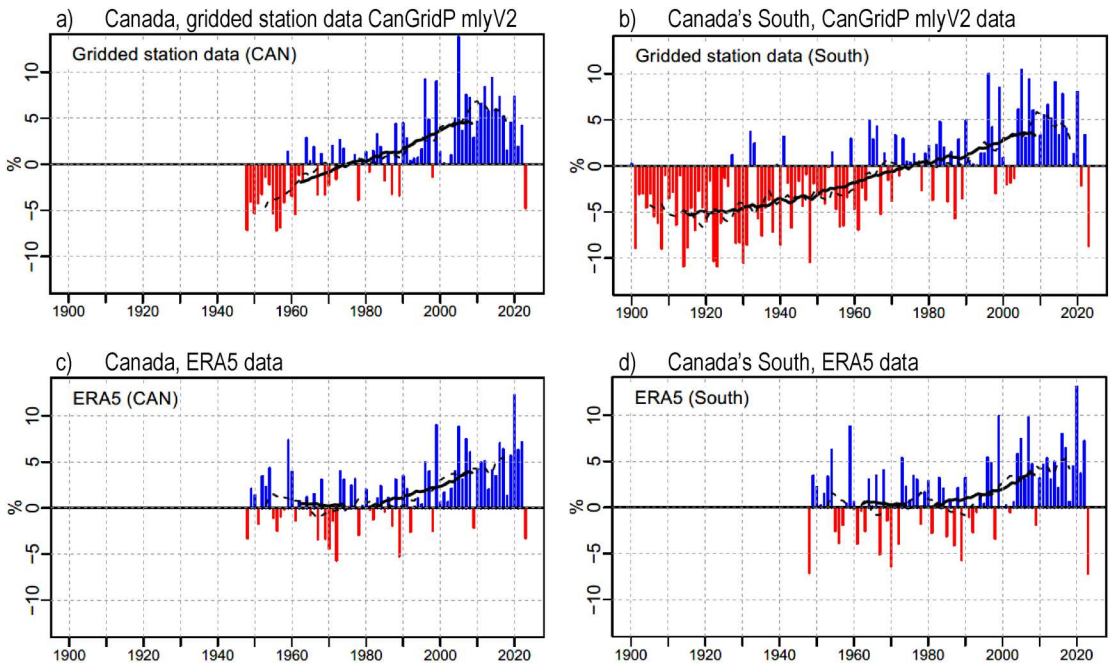

Fig. 10 Anomalies of the spatially averaged annual total precipitation amount expressed relative to its climatological mean amount for the 1961–1990 baseline period (baseline value). The dashed lines and thick solid lines are 11-year and 30-year running means, respectively. Anomalies of spatial means and corresponding baseline values are obtained from four different data sources, including CanGridP mlyV2 gridded station data (a, b) and ERA5 (c, d).

from CanGridP mlyV2 (sampling bias appears to cause an inhomogeneity in northern Canada in the end of November 1948, the effects of which was excluded by using the data since December 1948).

The results show that precipitation trends vary from region to region across Canada, and from season to season. Precipitation has increased in most areas from southern Nunavut to the Canadian Arctic Archipelago, and from Labrador to

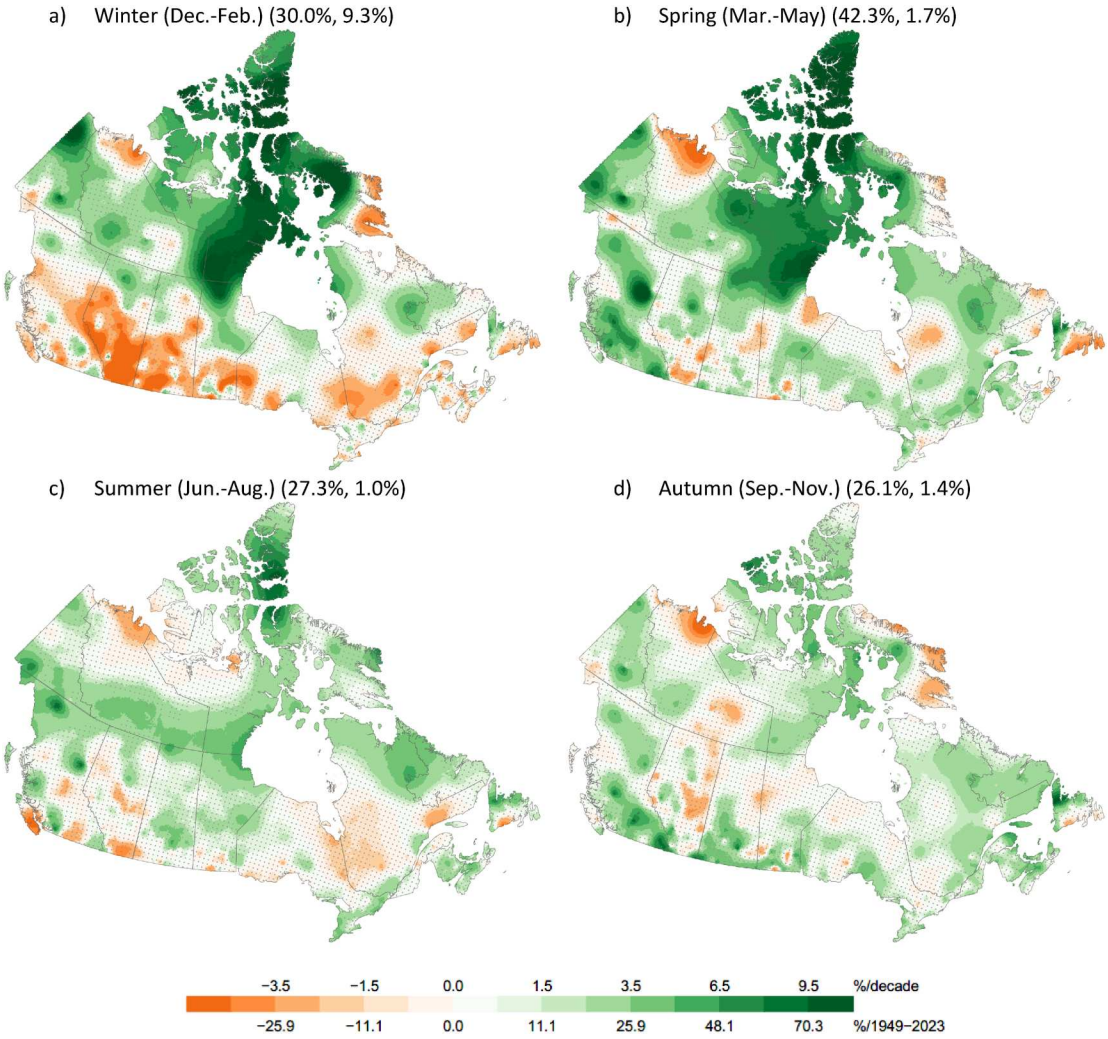

Fig. 11 The same as in Fig. 9, but for the seasonal trends over the period 1949–2023.

northeastern Quebec, in all seasons (especially winter and spring). It has also increased in a zonal band around 62°N in summer, and in most areas in British Columbia and along the St. Lawrence River in spring and autumn. The most outstanding seasonality of precipitation trends is seen in a broad band across southern Canada, where winter precipitation has decreased significantly without extensively significant changes in the other seasons (especially summer; Fig. 11). The best estimate of increase in the period between 1949 and 2023 is 9.7% for Canada as a whole, 18.9% for Canada's North, and 7.5% for Canada's South. Over the century-long period 1916–2023, precipitation in Canada's South has increased 10.7%.

In comparison with the previous CanGRD and CanGridP mlyV1 datasets, precipitation changes estimated from CanGridP mlyV2 scale with temperature changes in a way that better aligns with physically-based expectations, which suggest a scaling rate in mid-latitude land areas that is below the Clausius–Clapeyron rate of about 7% per °C of warming but above the global mean precipitation change scaling rate of 1–2% per °C of global warming. The CanGridP mlyV2 scaling rate for the change in Canada's mean precipitation over the period common to these datasets (1948–2012) is 5.5% per °C of warming in Canada, while the corresponding rates were unphysically high at 11.2% and 7.7% per °C for CanGRD and CanGridP mlyV1 respectively (Wang et al., 2023, also in supplementary Table S1). The unrealistic rates in the older datasets are largely due to the 1000+ cases of false zero or near-zero monthly precipitation amount arising from miscoded missing observations in the pre-1970 period (Section 3). During the gridding process, these false zero or near-zero precipitation amounts get interpolated to a large area when the station density is low, leading to estimated regional mean precipitation amounts that are biased low when data are sparce and the rapid increase seen in the 1960s in the regional mean series (Fig. 5, red dashed lines). While this source of bias estimates of Canada's precipitation trends has been substantially reduced, there is evidence that CanGridP mly V2 continues to be affected to

some extent by biases related to station density and changing data availability over time given that a significant inhomogeneity was detected in the end of November 1948 for northern Canada and whole Canada and that the estimated 1949–2023 scaling rate of 4.9% per °C of warming is noticeably higher than during the 1970–2023 period (2.6% per °C). Thus, while we have made use of a more extensive collection of sources of precipitation data (Section 2) to alleviate the challenge of insufficient data coverage, obtaining reasonably satisfactory results, there is room for further improvement.

Acknowledgements

The authors wish to thank Kaitlin DeBoer and Dr. Dan McKenney of Natural Resources Canada for ANUSPLIN modelling and extracting monthly precipitation estimates from the ANUPLIN surfaces, Rick Fleetwood for sharing his expert knowledge and useful information about CoCoRaHS observations, Rodney Chan for extracting data from the ECCC archive, and Hong Xu (an independent contractor with Environment and Climate Change Canada) for her contribution to the development and update of the AdjDlyRS dataset, the adjustment of the CoCoRaHS data and of Belfort and Fisher & Porter gauges data.

Disclosure statement

No potential conflict of interest was reported by the author(s).

Funding

This work was supported by the Environment and Climate Change Canada.

Supplemental data

Supplemental data for this article can be accessed online at https://doi.org/10.1080/07055900.2026.2617861.

Data availability statement

The source datasets used in this study are available in the Digital Archive of Canadian Climatological Data (https://climate.weather.gc.ca), the Canada Open Data Portal (http://open.canada.ca/data/en/dataset/d8616c52-a812–44ad-8754-7bcc0d8de305) for the Adjusted Daily Rain and Snowfall dataset version 2020, and CoCoRaHS data (CoCoRaHS – Community Collaborative Rain, Hail & Snow Network (https://www.cocorahs.org/ViewData/)). The new datasets produced in this study, CanHomP mlyV2, CanGridP mlyV2, and CanAdjP V2, will also be available at the Canada Open Data Portal (Open Government | Open Government, Government of Canada (https://open.canada.ca/en)) after this paper is published.

ORCID

Xiaolan L. Wang http://orcid.org/0000-0002-5656-5903
Vincent Y. S. Cheng http://orcid.org/0000-0003-3394-502X

References

Abbasnezhadi, K., & Wang, X. L. (2024). Comparison of gridding methods for precipitation over Canada and assessment of station and data density effects on gridding results. *Atmosphere-Ocean*, *62*(4), 320–346. https://doi.org/10.1080/07055900.2024.2394829

Bush, E., & Flato, G. (2019). About this report; Chapter 1. In E. Bush & D.S. Lemmen (Eds.), *Canada's Changing Climate Report* (pp. 7–23). Government of Canada, Ottawa, Ontario. https://doi.org/10.4095/314614

Cheng, V. Y. S., Wang, X. L., & Feng, Y. (2024). A quality control system for historical in situ precipitation data. *Atmosphere-Ocean*, *62*, 271–287. https://doi.org/10.1080/07055900.2024.23948

Hersbach, H., Bell, B., Berrisford, P., Hirahara, S., Horányi, A., Muñoz-Sabater, J., Nicolas, J., Peubey, C., Radu, R., Schepers, D., Simmons, A., Soci, C., Abdalla, S., Abellan, X., Balsamo, G., Bechtold, P., Biavati, G., Bidlot, J., Bonavita, M., … Thépaut, J. (2020). The ERA5 global reanalysis. *Quarterly Journal of the Royal Meteorological Society*, *146*(730), 1999–2049. https://doi.org/10.1002/qj.3803

Hutchinson, M. F., & Xu, T. (2013). *ANUSPLIN version 4.4 user guide*. Australian National University, Fenner School of Environment and Society. http://fennerschool.anu.edu.au/files/anusplin44.pdf

Ishii, M., Kamahori, H., Kubota, H., Zaiki, M., Mizuta, R., Kawase, H., Nosaka, M., Yoshimura, H., Oshima, N., Shindo, E., Koyama, H., Mori, M., Hirahara, S., Imada, Y., Yoshida, K., Nozawa, T., Takemi, T., Maki, T., & Nishimura, A. (2024). Global historical reanalysis with a 60-km AGCM and surface pressure observations: OCADA. *Journal of the Meteorological Society of Japan. Ser. II*, *102*(2), 209–240. https://doi.org/10.2151/jmsj.2024-010

Lee, J.-Y., Marotzke, J., Bala, G., Cao, L., Corti, S., Dunne, J. P., Engelbrecht, F., Fischer, E., Fyfe, J. C., Jones, C., Maycock, A., Mutemi, J., Ndiaye, O., Panickal, S., & Zhou, T. (2021). Future global climate: Scenario-based projections and NearTerm information. In V. Masson-Delmotte, P. Zhai, A. Pirani, S. L. Connors, C. Péan, S. Berger, N. Caud, Y. Chen, L. Goldfarb, M. I. Gomis, M. Huang, K. Leitzell, E. Lonnoy, J. B. R. Matthews, T. K. Maycock, T. Waterfield, O. Yelekçi, R. Yu, & B. Zhou (Eds.), *Climate change 2021: The physical science basis. Contribution of working group I to the sixth assessment report of the intergovernmental panel on climate change* (pp. 553–672). Cambridge University Press. https://doi.org/10.1017/9781009157896.006

MacDonald, H., McKenney, D. W., Wang, X. L., Pedlar, J., Papadopol, P., Lawrence, K., & Hutchinson, M. F. (2021). Spatial models of adjusted precipitation for Canada at varying time scales. *Journal of Applied Meteorology and Climatology*, *60*(3), 291–304. https://doi.org/10.1175/JAMC-D-20-0041.1

Martinez-Villalobos, C., & Neelin, J. D. (2019). Why do precipitation intensities tend to follow gamma distributions? *Journal of the Atmospheric Sciences*, *76*(11), 3611–3631. https://doi.org/10.1175/JAS-D-18-0343.1

Mekis, E., & Brown, R. (2010). Derivation of an adjustment factor map for the estimation of the water equivalent of snowfall from ruler measurements in Canada. *Atmosphere-Ocean*, *48*(4), 284–293. https://doi.org/10.3137/AO1104.2010

Nitu, R., Roulet, Y.-A., Wolff, M., Earle, M., Reverdin, A., Smith, C., Kochendorfer, J., Morin, S., Rasmussen, R., Wong, K., Alastrué, J., Arnold, L., Baker, B., Buisán, S., Collado, J. L., Colli, M., Collins, B.,

Gaydos, A., Hannula, H.-R., … Senese, A. (2018). WMO solid precipitation intercomparison experiment (SPICE) (2012–2015), instruments and observing methods report no. 131, World Meteorological Organization. Retrieved November 2022, from https://library.wmo.int/doc_num.php?explnum_id=5686

Slivinski, L. C., Compo, G. P., Whitaker, J. S., Sardeshmukh, P. D., Giese, B. S., McColl, C., Allan, R., Yin, X., Vose, R., Titchner, H., Kennedy, J., Spencer, L. J., Ashcroft, L., Brönnimann, S., Brunet, M., Camuffo, D., Cornes, R., Cram, T. A., Crouthamel, R., … Wyszy ski, P. (2019). Towards a more reliable historical reanalysis: Improvements for version 3 of the twentieth century reanalysis system. *Quarterly Journal of the Royal Meteorological Society*, 2876–2908. https://doi.org/10.1002/qj.3598

Smith, C. D., Mekis, E., Hartwell, M., & Ross, A. (2022). The hourly wind-bias-adjusted precipitation data set from the environment and climate change Canada automated surface observation network (2001–2019). *Earth System Science Data*, *14*(12), 5253–5265. https://doi.org/10.5194/essd-14-5253-2022

Vincent, L. A., Hartwell, M. M., & Wang, X. L. (2020). A third generation of homogenized temperature for trend analysis and monitoring changes in Canada's climate. *Atmosphere-Ocean*, *58*(3), 173–191. https://doi.org/10.1080/07055900.2020.1765728

Vincent, L. A., Zhang, X., Brown, R. D., Feng, Y., Mekis, E., Milewska, E. J., Wan, H., & Wang, X. L. (2015). Observed trends in Canada's climate and influence of low-frequency variability modes. *Journal of Climate*, *28*(11), 4545–4560. https://doi.org/10.1175/JCLI-D-14-00697.1

Wang, X. L. (2008a). Accounting for autocorrelation in detecting mean-shifts in climate data series using the penalized maximal *t* or *F* test. *Journal of Applied Meteorology and Climatology*, *47*(9), 2423–2444. https://doi.org/10.1175/2008JAMC1741.1

Wang, X. L. (2008b). Penalized maximal *F* test for detecting undocumented mean-shift without trend change. *Journal of Atmospheric and Oceanic Technology*, *25*(3), 368–384. https://doi.org/10.1175/2007JTECHA982.1

Wang, X. L., Chen, H., Wu, Y., Feng, Y., & Pu, Q. (2010). New techniques for the detection and adjustment of shifts in daily precipitation data series. *Journal of Applied Meteorology and Climatology*, *49*(12), 2416–2436. https://doi.org/10.1175/2010JAMC2376.1

Wang, X. L., & Feng, Y. (2013, July). *RHtestsV4 user manual*. Climate Research Division, Atmospheric Science and Technology Directorate, Science and Technology Branch, Environment Canada. 28 pp. https://github.com/ECCC-CDAS. https://doi.org/10.13140/RG.2.2.17309.17125

Wang, X. L., Feng, Y., Cheng, V., & Xu, H. (2023). Observed precipitation trends inferred from Canada's homogenized monthly precipitation dataset. *Journal of Climate*, *36*(22), 7957–7971. https://doi.org/10.1175/JCLI-D-23-0193.1

Wang, X. L., & Swail, V. R. (2001). Changes of extreme wave heights in northern hemisphere oceans and related atmospheric circulation regimes. *Journal of Climate*, *14*(10), 2204–2221. https://doi.org/10.1175/1520-0442(2001)014<2204:COEWHI>2.0.CO;2

Wang, X. L., Wen, Q. H., & Wu, Y. (2007). Penalized maximal *t* test for detecting undocumented mean change in climate data series. *Journal of Applied Meteorology and Climatology*, *46*(6), 916–931. https://doi.org/10.1175/JAM2504.1

Wang, X. L., Xu, H., Qian, B., Feng, Y., & Mekis, E. (2017). Adjusted daily rainfall and snowfall data for Canada. *Atmosphere-Ocean*, *55*(3), 155–168. https://doi.org/10.1080/07055900.2017.1342163

Zhang, X., Flato, G., Kirchmeier-Young, M., Vincent, L., Wan, H., Wang, X., Rong, R., Fyfe, J., Li, G., & Kharin, V. V. (2019). Changes in temperature and precipitation across Canada; Chapter 4. In E. Bush & D. S. Lemmen (Eds.), *Canada's Changing Climate Report* (pp. 112–193). Government of Canada. https://doi.org/10.4095/327811

Zhang, X., Vincent, L. A., Hogg, W. D., & Niitsoo, A. (2000). Temperature and precipitation trends in Canada during the 20th century. *Atmosphere-Ocean*, *38*(3), 395–429. https://doi.org/10.1080/07055900.2000.9649654